

Paper:

Rapid Generation of Surface Dimples Using End Milling

Shinichi Kogusu*, Takakazu Ishimatsu**, and Yasuhiko Ougiya**

*Industrial Technology Center of Nagasaki, 2-1303-8, Ikeda, Omura, Nagasaki 856-0026, Japan

E-mail: kogusu@tc.nagasaki.go.jp

**Dept. of Mechanical Systems Eng., Nagasaki University

1-14 Bunkyo-machi, Nagasaki 852-8521, Japan

[Received February 13, 2007; accepted June 4, 2007]

Structured surfaces on metal are often employed to enhance lubricating features, reduce the hydrodynamic drag force along wings and also decorate the metal surfaces for architectural ornament. It is important to note that only horizontal movements of a ball-end mill at high feed speed generate the indented surface on metal surfaces. In this paper we propose a technique to estimate the dimples generated on the metal surfaces using a machining center with an oval-end mill. Firstly, a technique to simulate the generating process of the dimples with the machining center is explained. The technique is effective in forecasting the geometry of the dimples with accuracy. Secondly, a technique to determine the cutting condition to generate the desired dimpled surface is proposed. The design specifications of the dimpled surface are the geometry of the dimples and the spacing between the dimples. The proposed technique was successfully used to decorate a metal surface.

Keywords: structured surfaces, machining center, oval-end mill, dimple texture

1. Introduction

Structured surfaces on the metal often yield superior features. Such structured surfaces on the metal are introduced to enhance lubricating features, reduce the hydrodynamic drag force along wings and decorate the metal surface [1–3]. Structured surfaces on the metal can be achieved by generating series of dimples on the target surface. Conventional industrial techniques to generate many dimples on the target surface are the photolithographic technique, the plastic deformation process and the milling technique. By using the photolithographic technique, fine dimples can be generated rapidly over a wide target surface area. A disadvantage of this technique however is that the technique requires expensive facilities. The plastic deformation process is a more practical technique, since the technique requires simple press working facilities. Conventional plastic deformation process generate dimples by pressing a dye onto the target surface. A disadvantage of this technique is that form accuracy and

roughness of the dimple is poor because of inability to control the plastic flow. A conventional milling technique can generate dimples over the target surface by a series of movements of a ball-end mill in the vertical and horizontal direction. Therefore, the milling technique requires significant multiplicity of vertical and horizontal movements to generate many series of dimples over a target surface area [4, 5].

It is important to note that only horizontal movements of the ball-end mill at high feed speed generate the indented surface on the metal surface. Tsutsumi et al. generated a quadratic and hexagonal pattern on a flat and curved surface using horizontal movements of a ball-end mill [6, 7]. Since the movement of the end mill of these milling processes is limited only in the horizontal direction, the generating process of the patterned indented surface can be simplified significantly. By reducing the depth of cut this generating process can produce dimples on the target surface. In order to estimate the geometry and the shape of these dimples generated by the horizontal movements of the end mill, a numerical technique is required. Furthermore, the technique should be applicable to the milling process using the oval-end mill since the introduction of such an oval-end mill offers a wider selection of types of dimples.

In this paper a technique to estimate the geometry and the shape of dimples generated by the horizontal milling process at high feed speed is proposed. In the proposed technique the oval-end mill is possible as well as the ball-end mill. An advantageous feature of this milling process is that the time required to generate the dimples is remarkably reduced. In order to make this milling process practical, the relationship between the desired dimple geometry and the cutting conditions are considered. Based on the milling experiments, it was confirmed that the desired dimples could be successfully generated. The calculated and actually generated geometry of the dimples correlated closely.

2. Concept to Generate Dimples

It is well known that dimples can be generated on a target surface by repeating the vertical and horizontal movements of an end mill. A disadvantage of this technique is



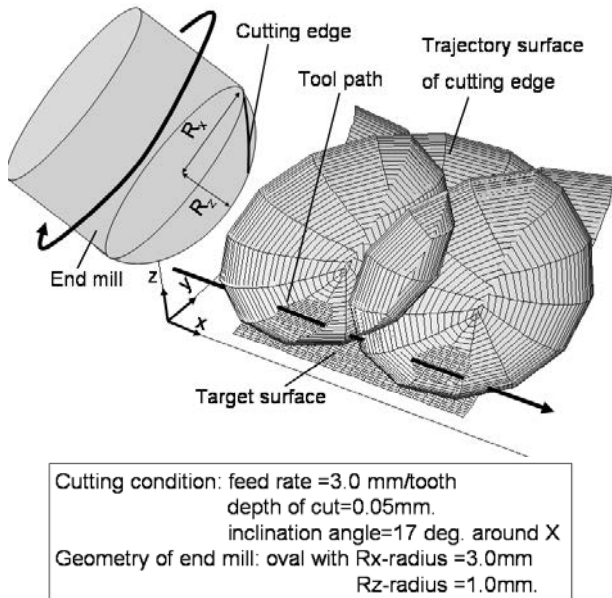


Fig. 1. Trajectory surface of cutting edge.

that the milling process requires significant time. In Fig. 1 a new concept to generate dimples using the milling process where the end mill is moved only in the horizontal direction is shown. The tool moves rightward. It should be noted that the feed rate is set to a significantly high value while the depth of cut set to a significantly low value. This figure shows the three-dimensional trajectory surface generated by the rotation and the horizontal movements of the cutting edge. The intersection of this three-dimensional surface and the target surface corresponds to the dimple generated. Therefore, the cutting conditions and also the shape of the cutting edge determine the three-dimensional geometry of the dimples generated. A feature of this technique is that the movement of the tool is only in the horizontal direction. Therefore, the processing time required to generate the desired dimples can be reduced significantly.

3. Analysis of Machined Surface Using Milling Process

A technique to obtain the three-dimensional trajectory of the cutting edge and the geometry of the generated dimple is proposed. In the followings the shape of the end mill is assumed to be oval in order to simplify the following explanation.

3.1. Numerical Model of Oval-End Mill

The numerical parameters to describe the geometry of the oval-end mill are shown in Fig. 2 where the x_t - y_t - z_t coordinate assumes the origin of the coordinate at the tip of the end mill. The three-dimensional geometry of the cutting edge is described in the x_t - y_t - z_t coordinates by the

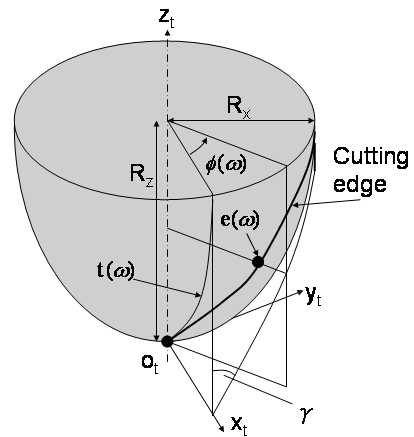


Fig. 2. Numerical model of oval-end mill.

following equation

$$\mathbf{e}(\omega) = \begin{bmatrix} e_x(\omega) \\ e_y(\omega) \\ e_z(\omega) \end{bmatrix} = \begin{bmatrix} t_x(\omega) \cos(\phi(\omega)) \\ t_x(\omega) \sin(\phi(\omega)) \\ t_z(\omega) \end{bmatrix} \quad (1)$$

$$\left(-\frac{\pi}{2} \leq \omega \leq 0\right)$$

$$\mathbf{t}(\omega) = \begin{bmatrix} t_x(\omega) \\ t_z(\omega) \end{bmatrix} = \begin{bmatrix} R_x \cos(\omega) \\ R_z \sin(\omega) + R_z \end{bmatrix} \quad \dots (2)$$

$$\phi(\omega) = \frac{\tan(\gamma)}{R_x} t_z(\omega) \quad \dots (3)$$

where ω is a scalar parameter to describe the position along the cutting edge. In this numerical model, the cutting edge is twisted linearly with the helix angle γ and the virtual surface generated by the rotation of the cutting edge is oval with the R_x and R_z radius.

3.2. Numerical Model of Tool Path

Assuming the target surface is represented by the position vector $\mathbf{w}(u, v)$, where the two-dimensional coordinates u and v are scalar parameters specifying the position on the target surface. The three-dimensional tool path on the target surface $\mathbf{b}(s)$ is shown in Fig. 3, which corresponds to the projection of the bottom line of the virtual groove which is generated by moving the end mill profile onto the target surface. Therefore, $\mathbf{b}(s)$ can be represented by,

$$\mathbf{b}(s) = \mathbf{w}(u(s), v(s)) \quad \dots (4)$$

The scalar parameter s is used to specify the position of the tool path.

3.3. Derivation of Trajectory Surface of Cutting Edge

In this section, the three-dimensional trajectory surface generated by the cutting edge during the milling process is explained.

Firstly, the three-dimensional surface position is denoted by the vector $\mathbf{g}(s, \omega)$, where s is a scalar parameter to specify a position on the three-dimensional tool path

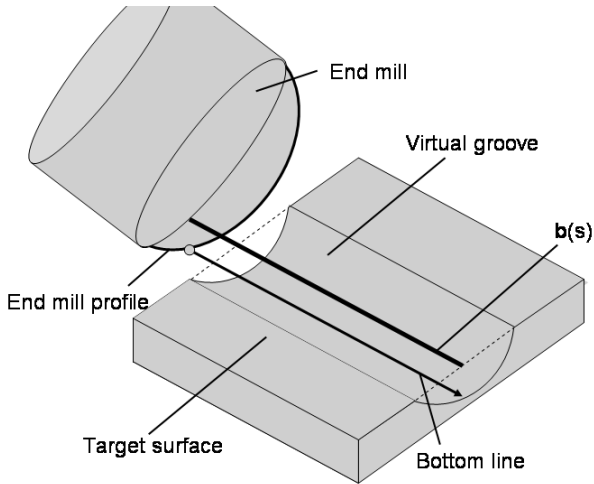


Fig. 3. Numerical model of tool path.

and ω is a scalar parameter to describe the position along the cutting edge.

By introducing the homogeneous transformation matrix, $\mathbf{g}(s, \omega)$ can be determined by [8]

$$\mathbf{g}(s, \omega) = [g_x(s, \omega) \quad g_y(s, \omega) \quad g_z(s, \omega)]^T \quad (5)$$

$$\begin{bmatrix} g_x(s, \omega) \\ g_y(s, \omega) \\ g_z(s, \omega) \\ 1 \end{bmatrix} = \mathbf{M}_1(s)\mathbf{M}_2(d_m)\mathbf{M}_3(\alpha)\mathbf{M}_4(\beta) \times \mathbf{M}_5(s) \begin{bmatrix} e_x(\omega) \\ e_y(\omega) \\ e_z(\omega) \\ 1 \end{bmatrix} \quad (6)$$

where $[e_x \ e_y \ e_z]^T$ denotes the shape of the cutting edge in the x_t - y_t - z_t coordinate system.

$\mathbf{M}_1(s)$ is the matrix to transform the workpiece coordinate system into the x_1 - y_1 - z_1 coordinate system, whose origin is set at $\mathbf{b}(s)$, the x axis is set to be a tangential line at $\mathbf{b}(s)$ and the z axis is normalized to the target surface. Therefore, $\mathbf{M}_1(s)$ becomes

$$\mathbf{M}_1(s) = \begin{bmatrix} \mathbf{x}_w(s) & \mathbf{z}_w(s) \times \mathbf{x}_w(s) & \mathbf{z}_w(s) & \mathbf{b}(s) \\ 0 & 0 & 0 & 1 \end{bmatrix} \quad (7)$$

$$\mathbf{x}_w(s) = \frac{d}{ds} \mathbf{b}(s) \quad (8)$$

$$\mathbf{z}_w(s) = \frac{\frac{\partial \mathbf{w}(u(s), v(s))}{\partial u} \times \frac{\partial \mathbf{w}(u(s), v(s))}{\partial v}}{\left| \frac{\partial \mathbf{w}(u(s), v(s))}{\partial u} \times \frac{\partial \mathbf{w}(u(s), v(s))}{\partial v} \right|} \quad (9)$$

$\mathbf{M}_2(d_m)$ represented by

$$\mathbf{M}_2(d_m) = \begin{bmatrix} 1 & 0 & 0 & 0 \\ 0 & 1 & 0 & 0 \\ 0 & 0 & 1 & d_m \\ 0 & 0 & 0 & 1 \end{bmatrix} \quad (10)$$

is the transformation matrix to offset the x_2 - y_2 - z_2 coordi-

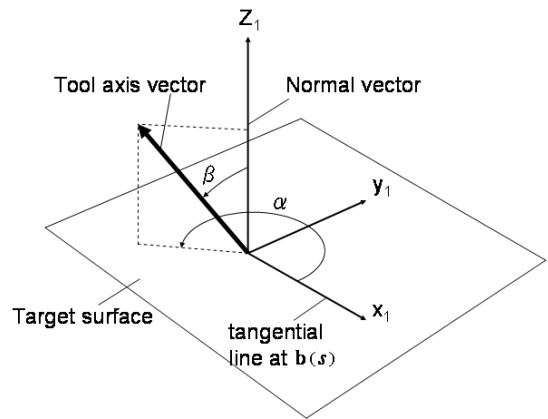


Fig. 4. Rotating angle α .

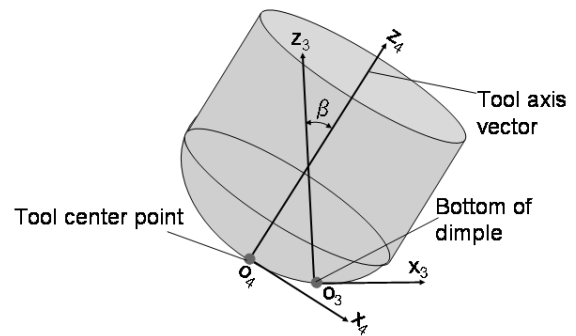


Fig. 5. x_4 - y_4 - z_4 coordinate system.

nate system in the z_1 axis with the displacement d_m , where d_m is the maximum depth of the generated dimple and the origin o_2 is set at the bottom of the dimple.

$\mathbf{M}_3(\alpha)$ is the transformation matrix represented by

$$\mathbf{M}_3(\alpha) = \begin{bmatrix} \cos(\alpha) & -\sin(\alpha) & 0 & 0 \\ \sin(\alpha) & \cos(\alpha) & 0 & 0 \\ 0 & 0 & 1 & 0 \\ 0 & 0 & 0 & 1 \end{bmatrix} \quad (11)$$

rotating the x_3 - y_3 - z_3 coordinate system around the z_2 axis with rotating angle α . Where the rotating angle α is the incline direction of the end mill around the vector normal to the target surface as defined in Fig. 4.

$\mathbf{M}_4(\beta)$ is the matrix to transform the x_4 - y_4 - z_4 coordinate system to the x_3 - y_3 - z_3 coordinate system represented by

$$\mathbf{M}_4(\beta) = \begin{bmatrix} \cos(\beta) & 0 & \sin(\beta) & -\cos(\beta) \cdot t_x(\omega_c) - \sin(\beta) \cdot t_z(\omega_c) \\ 0 & 1 & 0 & 0 \\ -\sin(\beta) & 0 & \cos(\beta) & \sin(\beta) \cdot t_x(\omega_c) - \cos(\beta) \cdot t_z(\omega_c) \\ 0 & 0 & 0 & 1 \end{bmatrix} \quad (12)$$

where β is the inclination angle around the y_3 axis and the origin O_4 is settled at the tool center point and the z_4 axis is settled to be equivalent to the tool axis vector as shown in Fig. 5.

The value ω_c in the above Eq. (12) is selected to satisfy the following equation

$$\omega_c(\beta) = -\text{arccot}(t_x \cdot \tan(\beta)/t_z) \quad (13)$$

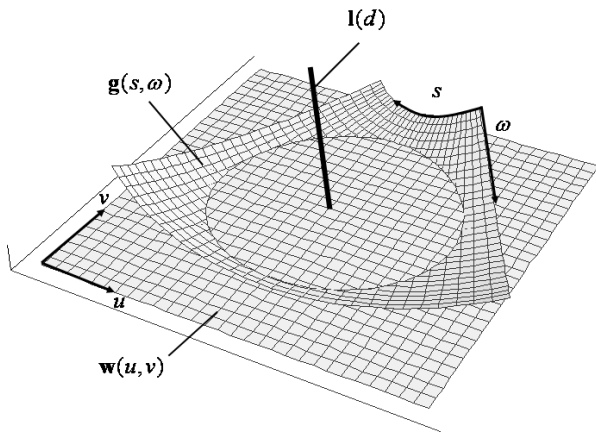


Fig. 6. Trajectory surface and target surface.

$M_5(s)$ is the transformation matrix represented by

$$M_5(s) = \begin{bmatrix} \cos(-2\pi \times \theta(s)) & -\sin(-2\pi \times \theta(s)) & 0 & 0 \\ \sin(-2\pi \times \theta(s)) & \cos(-2\pi \times \theta(s)) & 0 & 0 \\ 0 & 0 & 1 & 0 \\ 0 & 0 & 0 & 1 \end{bmatrix} \dots \dots \dots (14)$$

to rotate the x_5 - y_5 - z_5 coordinate system around the z_4 axis with a rotating angle $\theta(s)$ which is determined

$$\theta(s) = \frac{\int_{s_0}^s \left| \frac{d}{ds} \mathbf{b}(s) \right| ds}{f \cdot N_e} + \theta_0 \dots \dots \dots (15)$$

where f is the feed rate defined by the horizontal velocity of the end mill divided by rotation speed and the number of teeth N_e . θ_0 is the rotation angle of tool at the initial position of tool path s_0 .

By calculating $\mathbf{g}(s, \omega)$ at various s and ω values, the trajectory surface of the cutting edge can be obtained as shown in Fig. 6.

3.4. Determination of Geometry of Dimple

Since the trajectory surface of the cutting edge can be obtained as shown in Fig. 6, the geometry of the dimple can be determined by the intersection between the target surface and the trajectory surface of the cutting edge. The intersection can be obtained as follows:

The dimpled surface can be represented by the following equation

$$\mathbf{l}(d, u, v) = \mathbf{w}(u, v) - d\mathbf{n}(u, v) \dots \dots \dots (16)$$

where $\mathbf{n}(u, v)$ is unit vector normal to the target surface defined by

$$\mathbf{n}(u, v) = \frac{\frac{\partial \mathbf{w}(u, v)}{\partial u} \times \frac{\partial \mathbf{w}(u, v)}{\partial v}}{\left| \frac{\partial \mathbf{w}(u, v)}{\partial u} \times \frac{\partial \mathbf{w}(u, v)}{\partial v} \right|} \dots \dots \dots (17)$$

and d is the depth of the dimple. The intersection

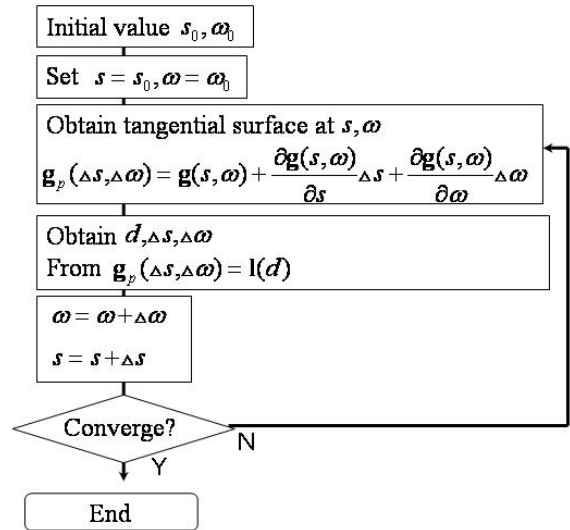


Fig. 7. Newton method to obtain intersection.

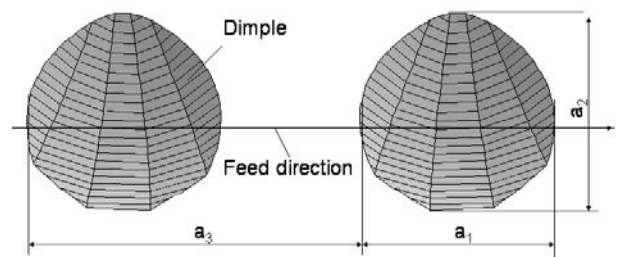


Fig. 8. Dimple geometry.

of the trajectory surface $\mathbf{g}(s, \omega)$ and the normal vector $\mathbf{l}(d, u_0, v_0)$ at point u_0, v_0 satisfies the following equation

$$\mathbf{l}(d, u_0, v_0) = \mathbf{g}(s, \omega) \dots \dots \dots (18)$$

The meaning of the above Eq. (18) can be readily understood as shown in Fig. 6. Solutions to satisfy Eq. (18) can be obtained by the Newton method as shown in Fig. 7. Therefore, calculating the intersection points at various u_0, v_0 the geometry of the dimpled surface can be determined.

4. Cutting Condition to Generate Desired Dimpled Surface

Considering the geometrical features of the milling process, a cutting condition to generate the dimpled surface with a desired geometry as shown in Fig. 8 can be determined following the procedures shown in Fig. 9. The rotation angle is assumed $\alpha = -90^\circ$. The procedures are explained as:

- (1) Supposing the desired dimples are arranged with an equal distance of a_3 in the feed direction. The shape of the dimple is oval-like with width a_1 in the feed direction and a_2 in the pick feed direction. In addition, Δa_1 and Δa_2

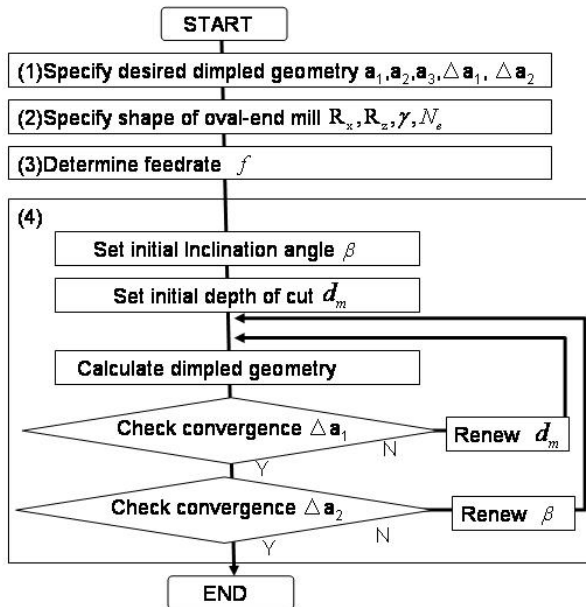


Fig. 9. Procedures to determine cutting condition.

Table 1. Cutting conditions 1.

Experiment No.	1	2	3	4
Desired width a_1 [mm]	1.4	1.4	1.4	1.4
Desired height a_2 [mm]	1.4	1.2	1.0	0.8
Depth of cut d_m [mm]	0.062	0.065	0.074	0.087
Rotation angle α [°]	-90	-90	-90	-90
Inclination angle β [°]	17	22	30	41
Feed speed [mm/min]	2400	2400	2400	2400
Spindle speed [1/min]	800	800	800	800

are the tolerance of width a_1 in the feed direction and a_2 in the pick feed direction.

(2) Specify the shape of oval-end mill with parameters R_x, R_z, γ, N_e , where R_z is required smaller than R_x .

(3) The feed rate is adjusted to $f = a_3$.

(4) The depth of cut d_m and the inclination angle β need to be determined using computer simulation so that the dimple becomes oval-like with a width of a_1 in the feed direction and a_2 in the pick feed direction. If the calculated width of a_1 of the dimple is smaller than the width of a_1 of the desired dimple, it is necessary to deepen the depth of cut d_m . If the calculated width of a_2 of the dimple is larger than that of the desired dimple, it is necessary to increase the inclination angle β .

5. Experiments

Experiments to generate dimples on the target surface were conducted. The target surface was a free-cutting flat brass plate. The dimples were generated with a three axis machining center using a cemented carbide oval-end mill (blade number $N_e = 1$). The shape of oval-end mill was $R_x = 3.0$ mm and $R_z = 1.0$ mm and the helix angle $\gamma = 0^\circ$.

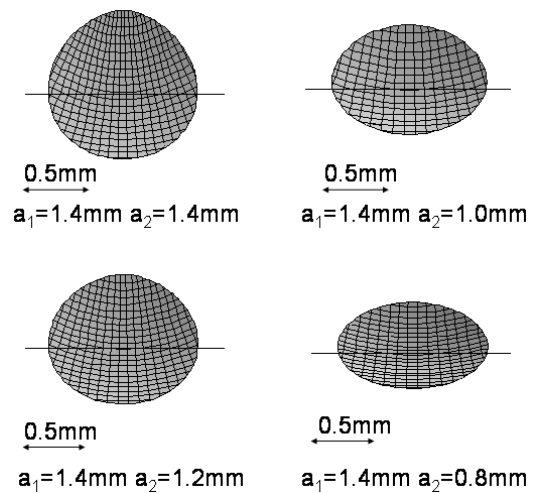


Fig. 10. Simulated dimples.

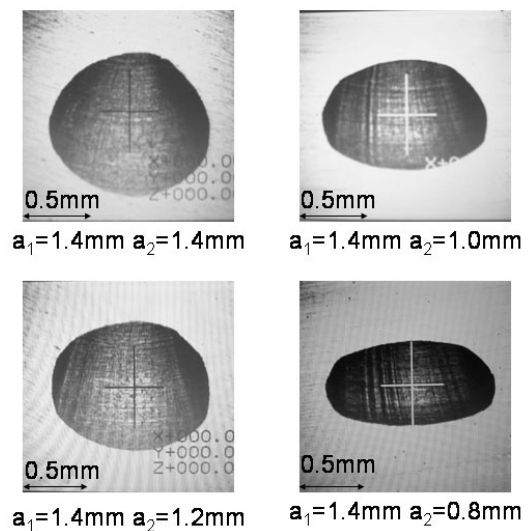


Fig. 11. Generated dimples.

Table 2. Simulated and Experimental data [mm].

Experiment No.	1	2	3	4
Desired width a_1	1.4	1.4	1.4	1.4
Desired height a_2	1.4	1.2	1.0	0.8
Simulated width a_1	1.400	1.400	1.400	1.400
Simulated height a_2	1.412	1.216	1.001	0.809
Experimental a_1	1.465	1.464	1.499	1.498
Experimental a_2	1.346	1.229	1.073	0.772

5.1. Experiment 1

A dimpled surface was generated with the width $a_1 = 1.4$ mm and the spacing $a_3 = 3.0$ mm. Only the height a_2 was varied to 1.4 mm, 1.2 mm, 1.0 mm and 0.8 mm. The cutting conditions were selected as shown in Table 1. Fig. 10 shows computer simulated dimples. Fig. 11 shows experimental dimple. In Table 2 the geometry of the simulated and experimental dimples are compared. The simulated data and the experimental data correlated well.

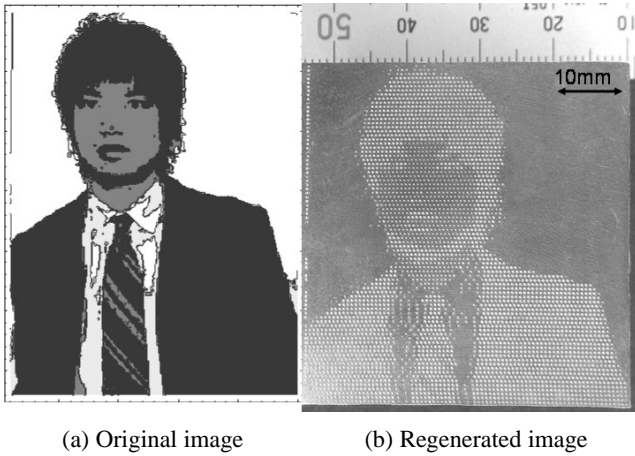


Fig. 12. Decoration of flat surface.

Table 3. Cutting conditions 2.

Experiment No.	1	2	3	4
Brightness	bright	semi-bright	semi-dark	dark
Desired width a_1 [mm]	NO	0.225	0.155	0.300
Depth of cut d_m [mm]	-0.030	0.038	0.010	0.038
Rotation angle α [°]	-90	-90	-90	-90
Inclination angle β [°]	50	50	50	50
Feed speed [mm/min]	2400	2400	1200	1200
Spindle speed [1/min]	2400	2400	2400	2400

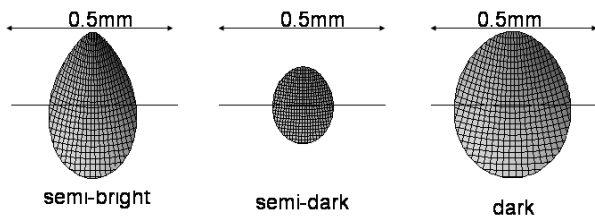


Fig. 13. Simulated geometries of dimples.

5.2. Experiment 2

In order to reveal the efficiency of the proposed technique a free-cutting brass flat plate were decorated with dimples using a ball-end mill with $R_x = 0.5$ mm as shown in Fig. 12. Four kinds of cutting conditions were selected as shown in Table 3. The simulated geometries of dimples are shown in Fig. 13. Under the first kind of cutting condition dimples were not generated. The geometry of dimples generated under the second and the forth cutting conditions were similar except the spacing between the dimples. These four kinds of cutting conditions were switched on the flat plate to regenerate the image of a man. The cutting conditions were switched based on the brightness of the target point. The relationship between the brightness and the cutting condition are also shown in Table 3. The number of the dimples to be generated per one second was 40 dimples/second.

6. Conclusions

In this paper a technique to estimate the geometry and the shape of dimples generated using a horizontal milling process at high feed speed is proposed. Features of the technique are as follows:

- (1) This technique is applicable to analyze the dimple generation process on a curved surface with an oval shaped cutting tool. The simulation is effective in estimating the geometry of the dimples with accuracy.
- (2) Using the simulation technique, the cutting condition can be determined to generate the desired dimpled surface in advance. The design specifications of the dimpled surface are the geometry of the dimples and the spacing between the dimples.
- (3) Dimples under various cutting conditions could be generated on the surface with various width and height. A free-cutting brass flat plate was decorated with dimples under four kinds of cutting conditions. The number of the dimples to be generated per one second was 40 dimples/second.

Acknowledgements

The authors would like to thank Mr. Kiyofumi Shigemori of the Industrial Technology Center of Kumamoto, Mr. Yoshihiro Tanigawa of The Industrial Technology Center of Fukuoka, Prof. Takanori Yazawa of Nagasaki University, Fumitaka Kimura of Keyence company Ltd. for their kind advice and help.

References:

- [1] I. Etsion, "State of the Art in Laser Surface Texturing," Journal of Tribology, Vol.127, Issue 1, pp. 248-253, 2005.
- [2] M. Weikert and F. Dausinger, "Surface structuring," Springer Berlin, Vol.96, 2004.
- [3] M. Lebbai, J. K. Kim, and M. M. F. Yuen, "Effects of Dimple and Metal Coating on Interfacial Adhesion in Plastic Packages," Journal of Electronic Materials, Vol.32, No.6, pp. 564-567, 2003.
- [4] T. Yazawa, M. Masuda, N. Ishibasi, and K. Syouzi, "Accuracy of Ridge on Dimple Milling," Division Report on Hyper Micro Texture Surface and Function Evaluation, Edited by Division of Manufacturing & Machine Tool in Japan Society of Mechanical Engineers, pp. 21-22, 2003.
- [5] Y. Takeuchi, "Micromilling," Journal of Japan Society for Precision Engineering, Vol.68, No.2, pp. 167-170, 2002.
- [6] H. Matsuda, H. Sasahara, M. Takizawa, and M. Tsutsumi, "Generation of Geometric Pattern on Plane Surface by Patch Division Milling," Journal of Japan Society for Precision Engineering, Vol.72, No.9, pp. 1123-1127, 2006.
- [7] A. Saito, X. M. Zhao, and M. Tsutsumi, "Control of Surface Pattern of Mold Generated by Ball-End Milling," Initiatives of Precision Engineering at the Beginning of a Millennium, 10th Int. Conf. on Prec. Eng. (ICPE), pp. 92-96, 2001.
- [8] R. P. Paul, "Robot Manipulators," Mathematics, Programming and Control, MIT Press, 1981.



Name:
Shinichi Kogusu

Affiliation:
Researcher, Industrial Technology Center of Nagasaki

Address:
2-1303-8 Ikeda, Omura, Nagasaki 856-0026, Japan

Brief Biographical History:

1999- Mitsubishi Electric Corporation
2001- Industrial Technology Center of Nagasaki

Membership in Academic Societies:

- The Japan Society of Mechanical Engineers (JSME)
 - The Japan Society for Precision Engineering (JSPE)
-



Name:
Yasuhiko Ougiya

Affiliation:
Associate Professor, Department of Mechanical Systems Engineering, Nagasaki University

Address:
1-14 Bunkyo-machi, Nagasaki 852-8521, Japan

Brief Biographical History:

1988- Nagasaki University

Main Works:

- "A Study of Noise and Vibration of Plastic Gears for Power Transmission," Proc. of The JSME International Conference on Motion and Power Transmissions MPT2001-Fukuoka, pp. 582-587, Nov. 2001.

Membership in Academic Societies:

- The Japan Society of Mechanical Engineers (JSME)
 - The Japan Society for Precision Engineering (JSPE)
 - Japanese Society for Engineering Education (JSEE)
-



Name:
Takakazu Ishimatsu

Affiliation:
Department of Mechanical System Engineering,
Nagasaki University

Address:
1-14 Bunkyo-machi, Nagasaki 852-8521, Japan

Brief Biographical History:

1978- Research Associate of Kyushu University
1981- Associate professor of Nagasaki University
1990- Professor of Nagasaki University

Main Works:

- "Development of an effective training machine using muscle activity information," Proc. of The 32nd Annual Conference of the IEEE Industrial Electronics Society (IECON'06), Paris, pp. 4534-4539, Nov. 2006.

Membership in Academic Societies:

- The Japan Society of Mechanical Engineers (JSME)
 - The Japan Society of Instrument and Control Engineers (SICE)
-